

# Antiviral Activity of an Isatin Derivative via Induction of PERK-Nrf2-Mediated Suppression of Cap-Independent Translation

Huifang M. Zhang,<sup>†,¶</sup> Huanqin Dai,<sup>‡,¶</sup> Paul J. Hanson,<sup>†</sup> Huidong Li,<sup>§</sup> Hui Guo,<sup>‡,¶</sup> Xin Ye,<sup>†</sup> Maged G. Hemida,<sup>†</sup> Luoqiang Wang,<sup>‡,⊥</sup> Yaojun Tong,<sup>‡,¶</sup> Ye Qiu,<sup>†</sup> Selina Liu,<sup>†</sup> Fengping Wang,<sup>†,¶</sup> Fuhang Song,<sup>‡</sup> Buchang Zhang,<sup>⊥</sup> Jian-Guo Wang,<sup>\*,§</sup> Li-Xin Zhang,<sup>\*,‡,⊥</sup> and Decheng Yang<sup>\*,†</sup>

<sup>†</sup>Department of Pathology and Laboratory Medicine, University of British Columbia, Institute for Heart and Lung Health, St. Paul's Hospital, Vancouver, BC V6Z 1Y6, Canada

<sup>‡</sup>Key Laboratory of Pathogenic Microbiology & Immunology, Institute of Microbiology, Chinese Academy of Sciences, Beijing, China

<sup>§</sup>State-Key Laboratory and Institute of Elemento-Organic Chemistry, Nankai University, Tianjin, China

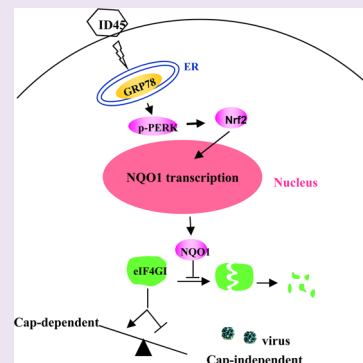
<sup>¶</sup>Graduate University, Chinese Academy of Sciences, Beijing, China

<sup>⊥</sup>School of Life Sciences, Anhui University, Hefei, China

<sup>#</sup>Department of Emergency, Harbin Medical University, Heilongjiang, China

## S Supporting Information

**ABSTRACT:** We report here an isatin derivative 45 (ID45) against coxsackievirus B3 (CVB3) replication, which was synthesized based on a high-throughput screen of a unique natural product library. ID45 showed the most potent anti-CVB3 activity among the four synthesized compounds. Treatment of cells with ID45 before or after infection significantly reduced viral particle formation, resulting in protection of cells from virus-induced apoptosis. In addition, ID45 treatment caused remarkable up-regulation of glucose-regulated protein 78 (GRP78), a hallmark of endoplasmic reticulum (ER) stress and an indicator of enhanced cell viability. In identifying the ER stress response pathway induced by ID45, we found that ID45 activated PKR-like ER protein kinase (PERK) but failed to up-regulate eIF2 $\alpha$  phosphorylation. Instead ID45 activated transcription factor Nrf2 (NF-E2-related factor-2), which is evidenced by its nuclear translocation and upregulation of its downstream target genes NQO1 (NAD(P)H quinone-oxidoreductase 1) and GCLM (glutamate-cysteine ligase, modifier subunit). This observation was further verified by using siRNAs of GRP78 or Nrf2, which blocked both the translocation of Nrf2 and up-regulation of its target genes, leading to aggressive viral replication and enhanced cell apoptosis. Finally, we found that ID45-induced up-regulation of NQO1 protected eIF4GI, a eukaryotic cap-dependent translation initiation factor, from cleavage by CVB3 protease and degradation by proteasomes. Taken together, our findings established that a novel antiviral mechanism of isatin derivative ID45 inhibits CVB3 replication by promoting cell survival through a PERK/Nrf2-dependent ER stress pathway, which benefits host cap-dependent translation but suppresses CVB3 cap-independent translation.



Coxsackievirus B3 (CVB3), an enterovirus in the *Picornaviridae* family, is the primary causal agent of viral myocarditis, particularly in children and young adolescents. This disease is often associated with sudden unexpected death.<sup>1</sup> Many synthetic compounds have been reported to inhibit enteroviruses.<sup>2,3</sup> Unfortunately, there is no approved antiviral drug for the treatment of acute enteroviral infections, including those against CVB3, in part because of the inadequacy of current chemical libraries in providing small molecules with sufficient activity against CVB3. Natural products have nevertheless historically played a valuable role in drug discovery and development because they occupy tremendous chemical structural space that is unmatched by any other small molecule families. A marine microbial extract library containing over 20,000 microbial extracts has been established in our laboratory and been screened for various biological activities.<sup>4,5,22</sup> Identifying beauvericin as an

antifungal potentiator and abyssomicins as potent anti-TB agents are good examples of the use of the library for drug discovery.<sup>5,6</sup>

CVB3 is a RNA virus, and its genome encodes 11 proteins including two viral proteases 2A and 3C.<sup>7</sup> The 5' end of the genome does not have a cap structure (a 7-methylguanosine triphosphate group); instead, it is covalently linked to a small viral protein VPg. This viral RNA also has an unusually long 5' untranslated region (5'UTR) harboring an internal ribosome entry site (IRES).<sup>8</sup> Thus, CVB3 RNA, unlike cellular mRNAs or many other viral genomes that start translation by a cap-dependent manner relying on the participation of cap-binding proteins and eukaryotic translation initiation factor 4GI

Received: October 9, 2013

Accepted: January 31, 2014

Published: January 31, 2014

(eIF4GI), initiates its translation by a cap-independent (IRES-driven) mechanism.<sup>9</sup>

Mammalian cells possess a signaling network that senses the accumulation of misfolded or unfolded proteins within the endoplasmic reticulum (ER)<sup>10</sup> and determines cell fate following exposure to stress signals including virus infections.<sup>11,12</sup> In addition, the ER membrane system is closely associated with the sites of picornaviral multiplication.<sup>13</sup> In response to ER stress, a coordinated, adaptive program called the unfolded protein response (UPR) is activated to adapt to stress signals targeting the ER. A master ER chaperon is the 78 kDa glucose regulated protein (GRP78).<sup>14</sup> Induction of GRP78 increases protein folding capacity, which represents a major survival arm of UPR and a host self-defense response. There are three major arms of the UPR network.<sup>15</sup> Among these, PERK-like ER protein kinase (PERK)-dependent signaling is critical for cell survival following the initiation of UPR. UPR-mediated PERK activation impedes protein translation via phosphorylation-dependent inhibition of eukaryotic translation initiation factor-2 $\alpha$  (eIF2 $\alpha$ ).<sup>16,17</sup> However, independent of its translational regulatory capability, PERK-dependent signals can also elicit the activation of pro-survival transcription factor Nrf2 (NF-E2-related factor-2), leading to cell survival.<sup>18</sup> A number of viruses including CVB3 have been shown to induce UPR during infection.<sup>11,12,19</sup> This response is a host self-defense mechanism against viral invasion. It is for this reason that the UPR pathway is an ideal target for antiviral drug screening and evaluation. In this study, based on our high throughput screening of the library, four isatin derivatives (ID) were synthesized. Antiviral evaluation using two well-established cell lines identified ID45 as a potent anti-CVB3 agent. We further revealed that ID45-induced up-regulation/activation of target genes enhances the stability of eIF4GI protein, a critical factor required for cap-dependent translation initiation of host mRNAs but a competitor against CVB3 RNA translation. These data suggest that ID45 inhibits CVB3 replication by activation of the pro-survival UPR pathway, leading to suppression of cap-independent translation of CVB3.

## RESULTS AND DISCUSSION

**Synthesis of Anti-CVB3 Isatin Derivatives Based on High Throughput Screening.** Isatin, a metabolite of marine bacteria in the embryos of some shrimps, enables the embryos to become remarkably resistant to infection by pathogenic fungus.<sup>20</sup> Isatin derivatives such as methisazone (marboran, MIBT, 1-methylisatin 3-thiosemicarbazone) were reported to inhibit vaccinia, cowpox, and herpes simplex virus infections.<sup>21,22</sup> Isatin and its derivatives were also identified as inhibitors of human mitochondrial monoamine oxidase B.<sup>23</sup> Furthermore, no toxicity is observed when using isatin. On the basis of this finding, we synthesized four new isatin derivatives, ID45, 48, 52, and 146 (Figure 1). Synthetic routes are shown in the Supplementary Figure S1. In testing antiviral effects using CVB3-infected cells, ID45 showed the strongest anti-CVB3 activity followed by methisazone<sup>21</sup> (a known ID control), ID52, and ID48. In contrast, ID146 seems to enhance CVB3 replication (Figure 2A). Meanwhile, we also used caspase-3 activation, an executive phase of cell apoptosis, as a criterion to demonstrate the strongest inhibition of pro-caspase-3 cleavage in the ID45-treated sample. The anti-CVB3 activity of ID45 was further tested using different MOIs (multiplicity of infection) and doses. Infections with 1 and 0.1 MOI all inhibited CVB3 replication. Considering the lower MOI infection will benefit the collection of enough cell lysates for analysis of signal transduction pathways in antiviral mechanism,

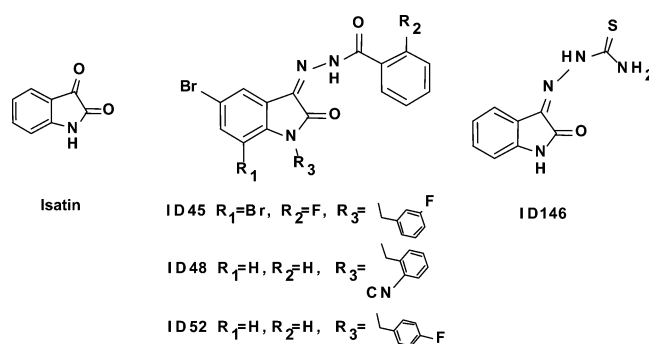


**Figure 1.** Chemical structure of isatin and its four derivatives.

we chose 0.1 MOI for this study. For the dose study, Figure 2B shows that ID45 treatment decreased the expression of viral VP1 protein in a dose-dependent manner, and the dose of 10  $\mu\text{M}$  ID45 reduced VP1 expression to an undetectable level. These data were further supported by a viral plaque assay (Figure 2C), showing dramatic reduction of CVB3 particle formation after treatment with ID45. The dose-dependent anti-CVB3 property of ID45 was also tested in HL-1 cardiomyocytes using similar conditions and produced similar results (Figure 2D,E).

On the basis of antiviral evaluation, we further confirmed ID45 structures by <sup>1</sup>H NMR, ESI-MS, and elemental analysis. <sup>1</sup>H NMR analysis data of ID45 is provided in Supplementary Figure S2. Compound ID45 was recrystallized from ethanol/dichloromethane to give yellow crystals suitable for X-ray single-crystal diffraction, the structure of which was determined using graphite monochromated Mo KR radiation (Supplementary Figure S3). Bond lengths, angles, and torsion angles of ID45 are listed in the Supplementary Table S1.

### Assays for Cytotoxicity and Time of Treatment of ID45.

To understand the mode of anti-CVB3 action and test for possible cytotoxicity caused by prolonged ID45 treatment, HeLa cells were treated with ID45 for 30 min, and then the compound was either removed by replacing fresh media without drug or retained for continuous treatment. The cells were then infected with CVB3 or sham-infected with phosphate-buffered saline (PBS). Antiviral activity and cytotoxicity were detected by Western blot for VP1 and MTS cell viability assay, respectively, at 16 h post infection (pi). Figure 3A shows that CVB3 VP1 levels in ID45-removed cells were slightly higher than that in ID45-retained cells, indicating that treatment with ID45 for 30 min is long enough for drug internalization and full function. This also indicates that longer treatment does not increase cytotoxicity. As CVB3 infection causes cell apoptosis,<sup>24</sup> we next investigated whether the antiviral activity of ID45 is associated with the induction of cell death. We first found that treatment with ID45 in the sham-infected controls (Figure 3A, lanes 1 and 2) did not cause cleavage of pro-caspase-3, indicating that the compound is not toxic and ID45 itself cannot induce cell apoptosis. We further found that cleaved caspase-3 in ID45-treated cells (lanes 4 and 6) is less than that in DMSO-treated cells (lanes 3 and 5), indicating again that ID45 inhibits cell apoptosis and benefits cell survival during CVB3 infection. This conclusion is supported further by the cell viability assay, which demonstrated that in ID45-treated/CVB3 infected cells, either removal or retention of the compound could result in a high rate (81–86%) of cell viability. Specifically, there was a 17–23% increase as compared to the corresponding control cells treated with DMSO (Figure 3B).

To evaluate the potential for future clinical trial, we mimicked the natural conditions for the treatment of the existing infection,

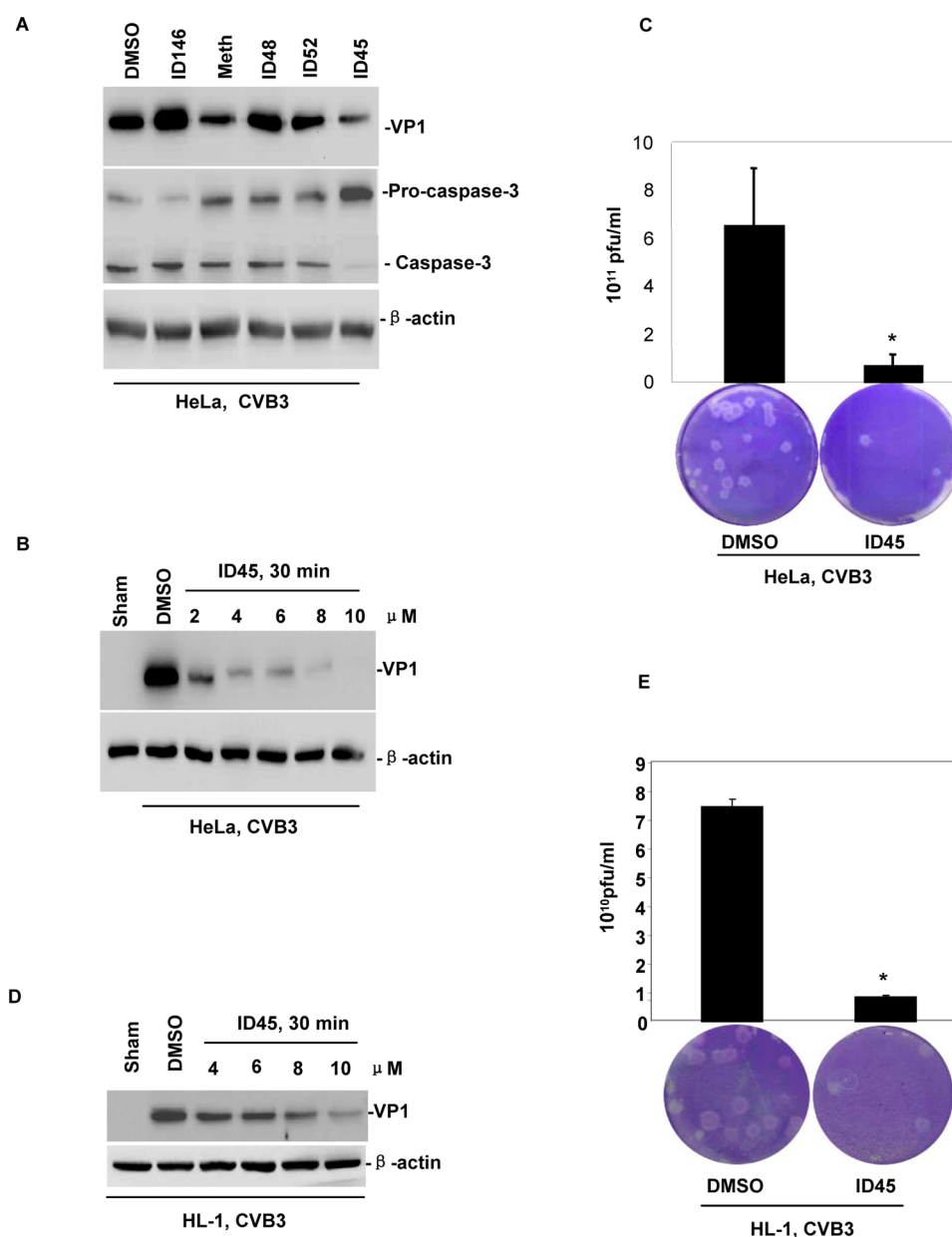


**Figure 2.** *In vitro* validation of anti-CVB3 activity of isatin derivatives. (A) *In vitro* screen. HeLa cells were treated with four new isatin derivatives (ID146, ID52, ID48, and ID45, respectively) at 10  $\mu$ M for 30 min and then infected with CVB3 at 0.1 MOI for 16 h. This is the infection condition used throughout this study unless otherwise specified. Methisazone- and DMSO-treated cells were used as positive and negative controls, respectively. Antiviral activity was evaluated by Western analysis of CVB3 VP1 protein production and cleavage of pro-caspase 3.  $\beta$ -Actin was used as an equal loading control. (B) Dose testing. HeLa cells were treated with ID45 at indicated doses and then infected with CVB3. Cell lysates were collected for Western analysis using a VP1 antibody. (C) Plaque assay. CVB3 particles were measured by viral plaque assay using supernatants from 10  $\mu$ M ID45-treated and CVB3-infected cells. (D) Validation in HL-1 cardiomyocytes. HL-1 cells were cultured in Claycomb medium and treated with ID45 at different doses and then infected with CVB3. Anti-CVB3 activity was validated by Western analysis of VP1. (E) Plaque assay. CVB3 particles were measured by plaque assay using supernatants from HL-1 cells treated with 10  $\mu$ M ID45 ( $n = 3$ ,  $p < 0.05$ ).

i.e., treatment of the cells after CVB3 infection. We treated the cells with ID45 at 2 or 6 h after viral infection and found that the levels of VP1 reduction as well as the activation of caspase-3 were similar to that of cells treated for 30 min prior to infection (Figure 3C). This anti-CVB3 activity independent of time of treatment was further verified by evaluation using HL-1 cardiomyocytes (Figure 3D). We further showed that the reduction of VP1 expression (Figure 3D) was due to corresponding promotion of HL-1 cell viability (Figure 3E). In the cell viability assay, comparing to sham-infected control, cells pretreated with ID45 for 30 min and then infected with CVB3 showed 78% cell

survival, which is almost the same as that of the cells treated at 6 h pi. These data suggest that the antiviral effect of ID45 is independent of the time for addition of the compound. Most of the previous antiviral drugs inhibit viral replication via their pro-apoptotic activity, which kills the host cells supporting viral replication. In a cytotoxicity assay, we noticed that the sham-infected cells treated with ID45 did not show activation of caspase-3; ID45 is not only nontoxic to the cells but also enhances cell viability.

**ID45 Treatment Induces GRP78 Up-regulation and UPR in Both Dose-Dependent and Time-Dependent**

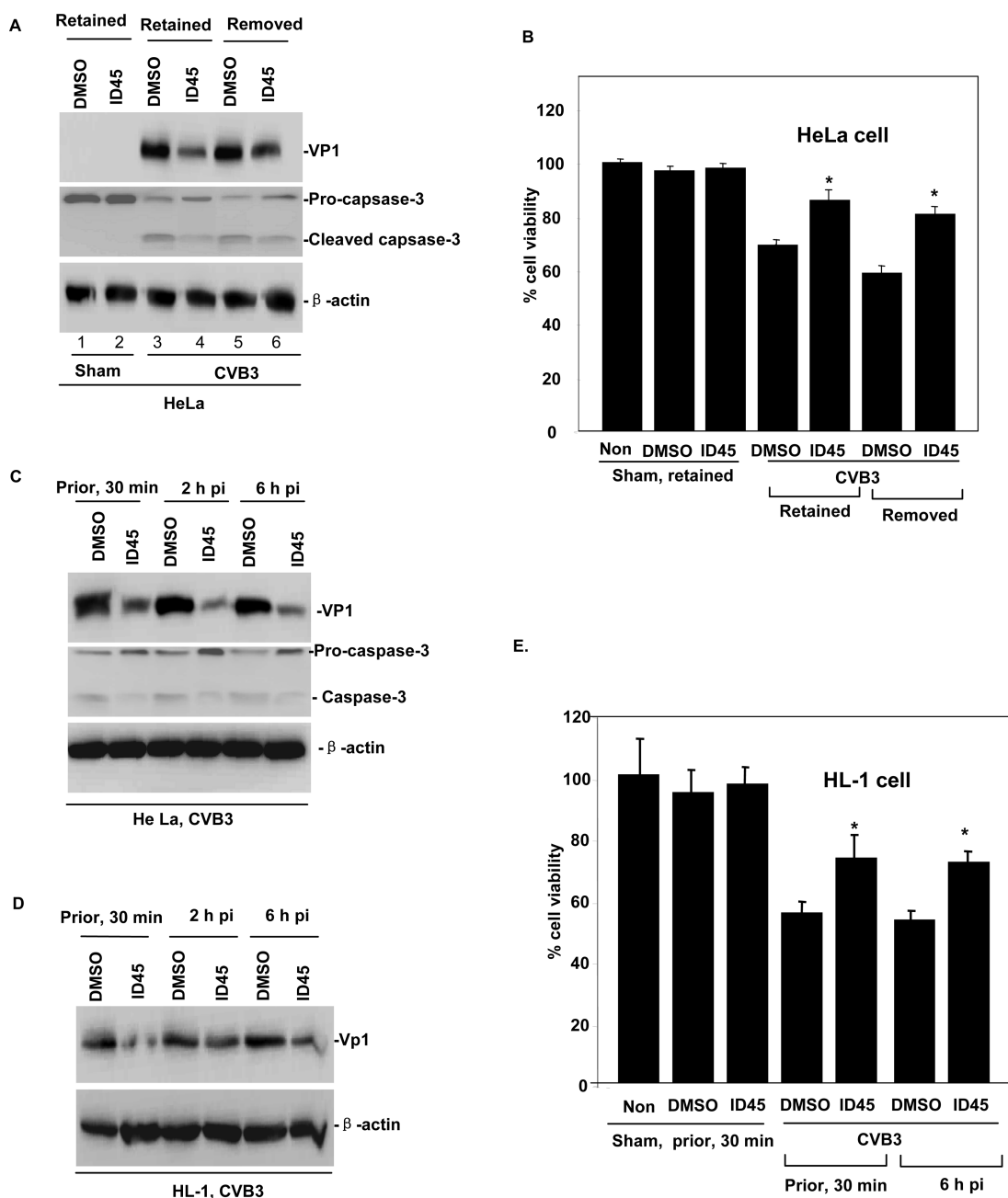


**Figure 3.** Assays for cytotoxicity and time of treatment. (A) HeLa cells were treated with ID45 for 30 min, and the drug was either removed by replacing the medium or retained for continuing treatment. The cells were then infected with CVB3 or sham-infected. Antiviral activity was determined by Western analysis of VP1 and cleavage of pro-caspase-3 as described in Figure 2. (B) Cytotoxicity of ID45 was evaluated with a MTS cell viability assay using HeLa cells treated as described in panel A. Cell viability of nontreated/sham-infected cells was defined as 100% (control). Other data are presented as percentage of the control ( $n = 3$ ,  $p < 0.05$ ). Time of treatment assay. HeLa cells (C) or HL-1 cells (D) were treated for 30 min prior to or 2 or 6 h pi CVB3 infection. Anti-CVB3 evaluation was conducted by Western analysis as described above. Cytotoxicity of ID45 was evaluated with the MTS cell viability assay using HL-1 cells (E) treated with ID45 for 30 min prior to or 6 h pi. The additional controls are cells nontreated/sham-infected as indicated. Cell viability of the samples were determined as described in panel B ( $n = 3$ ,  $p < 0.05$ ).

**Manners.** While studying the underlying mechanism by which ID45 promotes cell survival and inhibits CVB3 replication, we first speculated that the ERK and/or PI3K/Akt pathways may be involved in the pro-survival activity of ID45. However, we failed to detect the activation of these two pathways (data not shown). As our previous study demonstrated that CVB3 infection induces GRP78 up-regulation and subsequent activation of UPR, a host survival strategy,<sup>19</sup> we asked whether ID45-induced cell survival is due to its ability to up-regulate GRP78 and enhance UPR.<sup>30,31</sup> To address this question, we treated cells with ID45 at doses

from 2 to 10  $\mu\text{M}$  for 30 min. We also treated cells with ID45 at 10  $\mu\text{M}$  for different durations ranging from 0.5 h to overnight. We found that ID45 did induce up-regulation of GRP78 and cell morphology changes in both dose-dependent and duration-dependent manners, as detected by Western analysis (Figure 4A,B) and phase-contrast microscopy (Figure 4C). All these data indicate that under the treatment of ID45 overnight most of the cells showed the round-up shape and reduced size compared to DMSO-treated cells (Figure 4C panel d). However, the detection of caspase-3 activation did not show pro-caspase-3

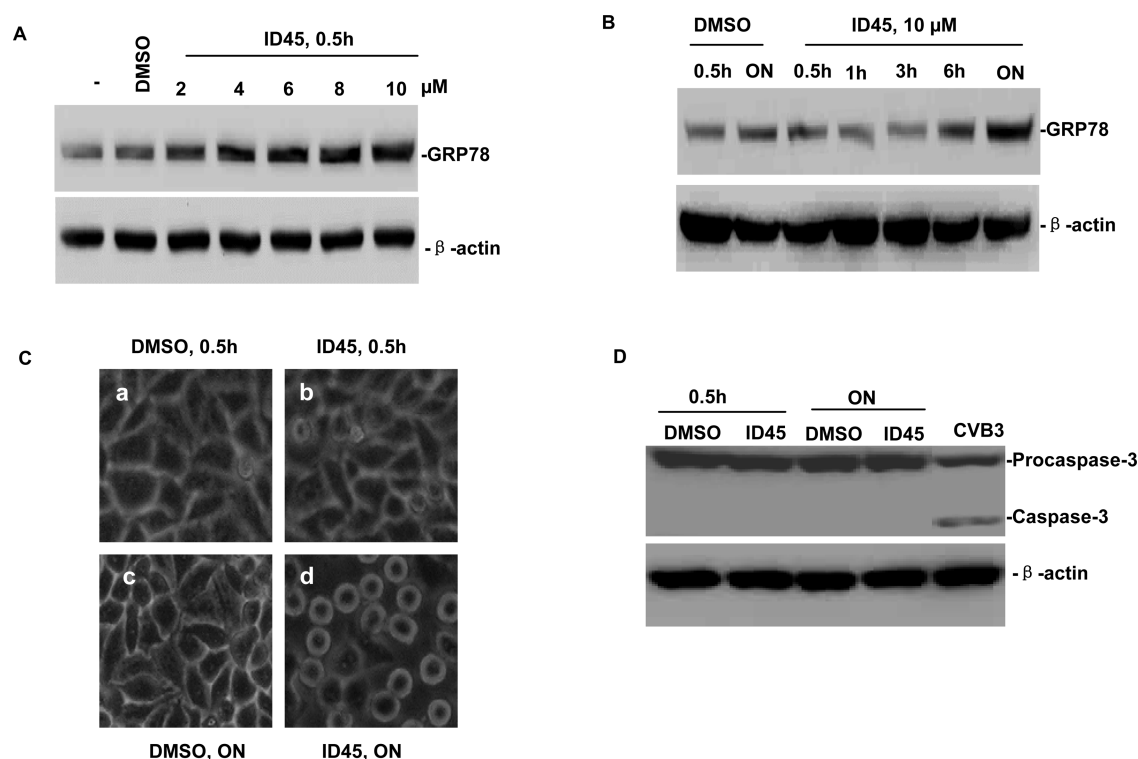


**Figure 4.** ID45 up-regulates GRP78 and induces UPR in both dose- and time-dependent manners. (A) HeLa cells were treated with ID45 at indicated doses for 30 min. Cell lysates were collected for Western analysis of GRP78 expression. (B) HeLa cells were treated with ID45 for the indicated time courses. GRP78 expression was determined by Western blot.  $\beta$ -Actin was an equal loading control. (C) The cell morphological changes were observed after 30 min or overnight (ON) treatment by phase contrast microscopy. (D) Pro-caspase-3 cleavage was detected by Western blot. CVB3-infected cell was used as a positive control.

cleavage in these cells (Figure 4D), suggesting that this morphology change is not due to cell apoptosis but due to cell responses to ER stress.

**Silencing of GRP78 with siRNAs Relieves ID45-Induced UPR and Attenuates CVB3 VP1 Reduction.** To further verify that ID45-induced antiviral effect occurs through induction of GRP78 and activation of UPR, we transfected cells with siRNAs targeting GRP78 and then treated with ID45 but without CVB3 infection. To confirm that silencing of GRP78 would suppress ID45-induced inhibition of VP1 expression, HeLa cells were transfected with GRP78 siRNAs, treated with ID45, and then infected with CVB3. Western analysis (Supplementary Figure S4C) showed that silencing of GRP78 with siRNAs reduced GRP78 expression. However, only when cells were transfected with scrambled siRNA and treated with ID45, the reduction of the VP1 protein production reached the lowest level (lane 4) compared to other treatments. These data suggest that ID45-induced VP1 reduction is through up-regulation of GRP78 and activation of the pro-survival pathway of ER stress response.

**ID45 Induces Cell Survival via PERK-Nrf2 but Not PERK-eIF2 $\alpha$  Pathway of UPR.** Having demonstrated that ID45 could promote cell survival via activating the GRP78-mediated UPR, our next step was to identify the specific branch of the UPR pathway that leads to cell survival. During ER stress, PERK activation has been recognized as one of the central mediators determining cell fate during ER stress. Although PERK activation can suppress translation of certain proteins, it can also promote translation of certain proteins involved in cell growth or death. In addition to inducing cell apoptosis via phosphorylation of eIF2 $\alpha$ <sup>25</sup> and subsequent up-regulation of proapoptotic transcription factor CHOP,<sup>26</sup> p-PERK can also directly activate pro-

survival transcription factor Nrf2<sup>18</sup> by up-regulation and nuclear translocation of this protein.<sup>27</sup> To reveal the underlying signal pathway activated by ID45, HeLa cells were treated with ID45 for 16 h, and cellular proteins were extracted for Western analysis. Figure 5A shows that ID45 induced up-regulation of phosphorylated PERK (p-PERK) following GRP78 induction of UPR but did not significantly change the levels of phosphorylated eIF2 $\alpha$  (p-eIF2 $\alpha$ ) and total eIF2 $\alpha$ . This implies that ID45-induced UPR cannot induce the p-eIF2 $\alpha$ -mediated apoptosis pathway. Thus, we turned our attention to detect the up-regulation of Nrf2, a transcription factor that can be activated directly by p-PERK.<sup>18</sup> We found that Nrf2 was significantly up-regulated after ID45 treatment in both HeLa cells and cardiomyocytes. This Nrf2 activation was further verified by the facts that (i) there was significant up-regulation of the target genes, NQO1 (NAD(P)H quinone-oxidoreductase 1) and GCLM (glutamate-cysteine ligase, modifier subunit) (Figure 5A) and (ii) similar results were obtained by experiments using murine HL-1 cells (Figure 5B). Since the antibody against human GCLM did not work for murine HL-1 cells, we excluded this protein from the detections in HL-1 cells.

Nrf2 activity is usually suppressed by Keap1 protein in unstress conditions through interactions to form an Nrf2-Keap1 complex.<sup>28</sup> To determine if Keap1 protein is involved in ID45-mediated regulation of Nrf2 expression, we knocked down Keap1 with specific siRNAs and then treated the cells with ID45. Supplementary Figure S5 shows that silencing Keap1 with siRNAs increased Nrf2 levels compared to the cells treated with scrambled control siRNAs. However, when comparing the ID45-treated cells with the DMSO-treated samples, although the Nrf2 levels were dramatically increased by ID45 treatment in

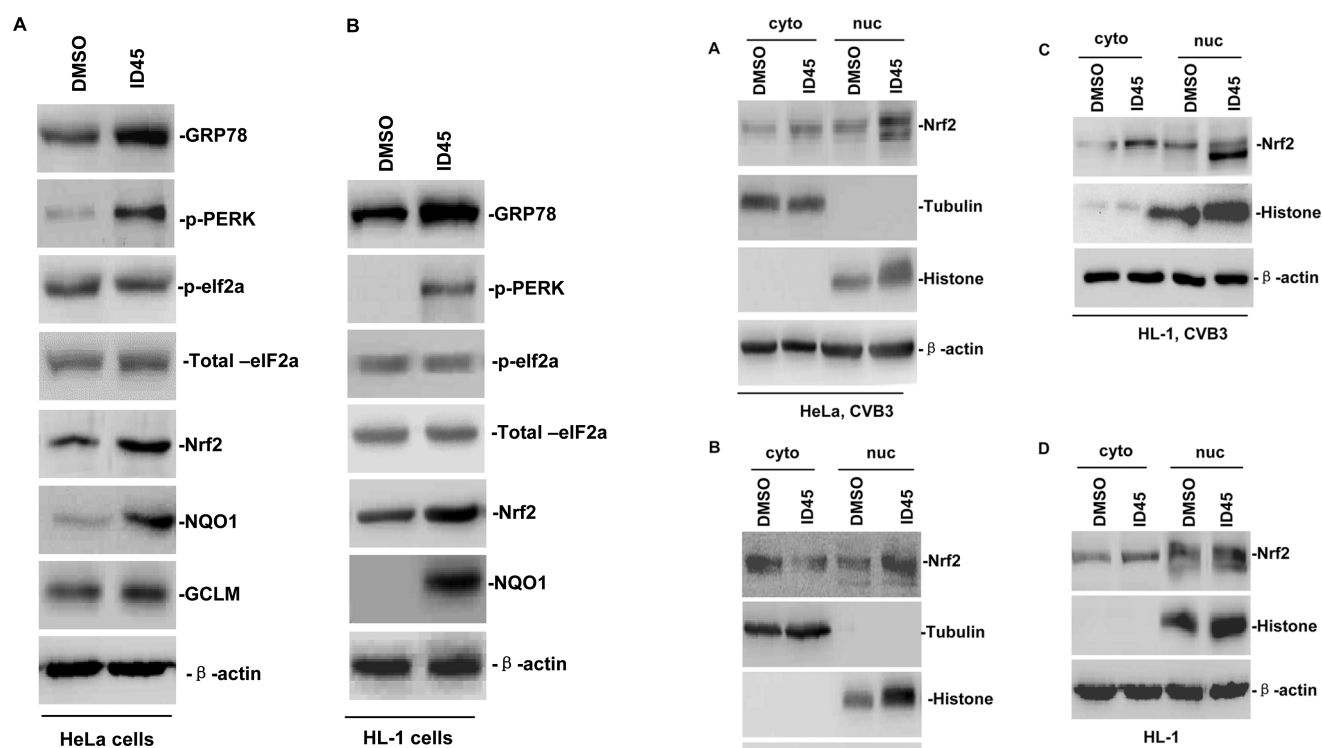


**Figure 5.** ID45-induced GRP78 up-regulation activates PERK-Nrf2 pathway of UPR. HeLa cells (A) and HL-1 cells (B) were treated with ID45 as described above. Whole cell lysates were collected for Western analysis to detect up-regulation of GRP78 and Nrf2, phosphorylation of PERK and eIF2 $\alpha$ , total level of eIF2 $\alpha$ , as well as up-regulation of Nrf2 and its target genes NQO1 and GCLM.  $\beta$ -Actin was used as an equal loading control.

scrambled siRNA-treated cells, this increase was not obvious in Keap1 siRNA-treated samples. In addition, NQO1 expression level also showed a similar pattern as that of Nrf2 in the corresponding cells. These data suggest that ID45-induced Nrf2 activation is largely through the induction of dissociation of Nrf2-Keap1 complex.

#### ID45 Treatment Induces Nrf2 Nuclear Translocation.

Nrf2 has been well studied in antioxidative stress signaling. During oxidative stress, Nrf2 dissociates from the Keap1/Nrf2 complex and is transported into the nucleus, where it promotes expression of its downstream target genes involved in cell growth.<sup>27</sup> Thus, the function of Nrf2 in cytoprotection is documented in promoting longevity,<sup>29</sup> disease prevention,<sup>30,31</sup> and shaping immune response to hepatitis B virus infection.<sup>32</sup> The ID45-induced nuclear translocation of Nrf2 protein was demonstrated in both CVB3- and sham-infected HeLa cells by Western analysis using cytosolic and nuclear proteins. The purity of these proteins was monitored by detecting tubulin and histone protein, respectively. Figure 6A shows that ID45-treated cells showed an increased amount of Nrf2 in nuclear extract compared to that in the cytosolic fraction. A similar result was observed in PBS sham-infected cells (Figure 6B). It seems that CVB3 infection enhanced ID45-induced Nrf2 nuclear import. These data were further solidified in HL-1 cells (Figure 6C,D). To directly observe the up-regulation and translocation of Nrf2 in the cells, immunocytochemical staining of the proteins was conducted, and the result of this showed that Nrf2 protein translocated to the nucleus after ID45 treatment overnight (Figure 6E).

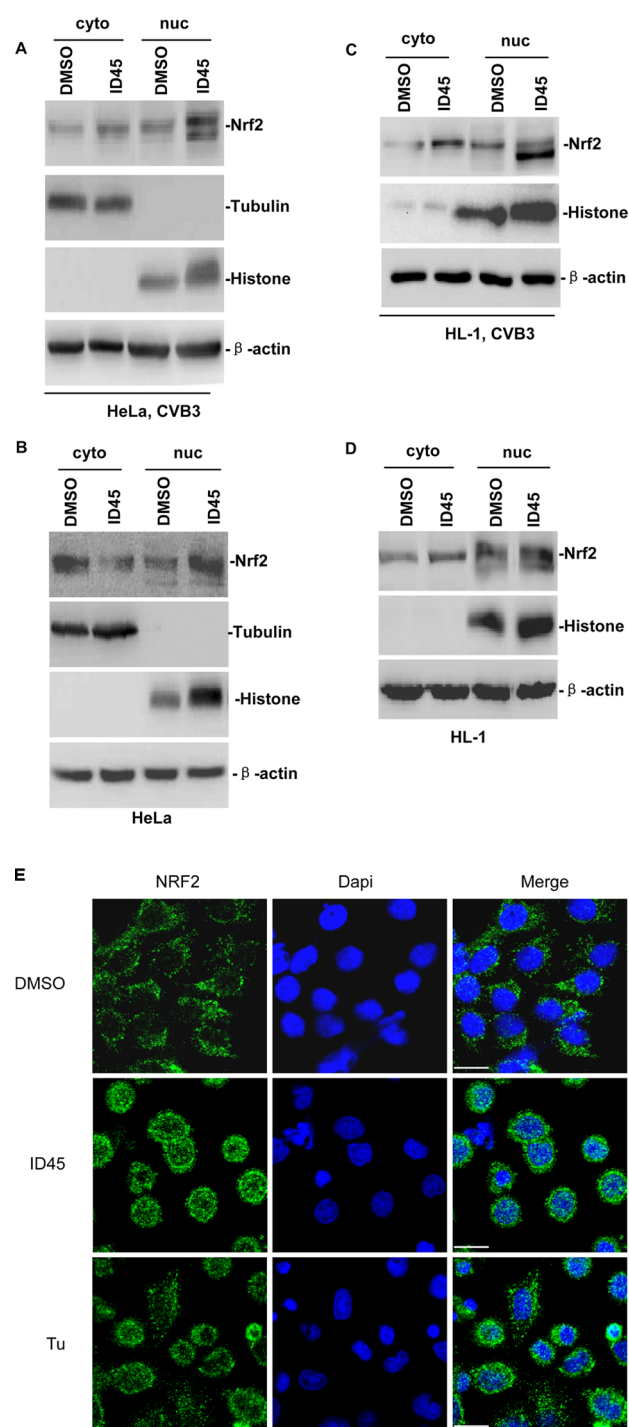


**Figure 6.** ID45 treatment induces Nrf2 nuclear translocation. HeLa cells were treated with ID45 and then infected with CVB3 (A) or sham-infected with PBS (B). The cytosolic and nuclear proteins were isolated, and the Nrf2 protein distribution in these fractions was detected by Western analysis.  $\alpha$ -Tubulin and histone were used for purity control of cytosolic and nuclear extractions, respectively.  $\beta$ -Actin was the loading control. The experiment was repeated to verify the findings using HL-1 cells and the corresponding data are shown in panels C and D, respectively. (E) Immunostaining. HeLa cells culturing on glass coverslips were treated with ID45 overnight. The cells were stained with an anti-Nrf2 primary antibody and then a green-fluorescent Alexa Fluor 488 dye-conjugated second antibody. The nuclei were counterstained with DAPI. Nrf2 protein distribution in cytosol and nucleus was visualized by confocal microscopy. HeLa cells treated with tunicamycin (1  $\mu$ g/mL) overnight were visualized as a control.

### Silencing GRP78 or Nrf2 with siRNAs Attenuates ID45-Induced Nrf2 Up-regulation and Nuclear Translocation.

To further confirm that ID45-induced up-regulation of Nrf2 and its target gene NQO1 as well as the subsequent nuclear translocation of Nrf2 is due to GRP78-mediated UPR, total cellular proteins were isolated from HeLa cells transfected with siRNAs targeting GRP78 or Nrf2 and then treated with ID45. Western analysis showed that GRP78 siRNAs suppressed both GRP78 and Nrf2 expression, while Nrf2 siRNAs suppressed only Nrf2 expression compared to GRP78 siRNA. These data imply that GRP78 is located upstream of Nrf2 in this pathway. The GRP78-mediated activation of Nrf2 was further solidified by the suppression of its target gene NQO1 expression via siRNA silencing of either Nrf2 or GRP78 (Supplementary Figure S6A). To further demonstrate the activation of Nrf2 by observation of its nuclear translocation, cytosolic and nuclear proteins were extracted. Western analysis showed that both siRNAs attenuated the gene expression and nuclear translocation of Nrf2 (Supplementary Figure S6B). These data suggest that ID45 induces UPR-mediated cell survival signaling via activation of GRP78 and induction of Nrf2 nuclear translocation.

**Silencing Nrf2 Suppresses Antiviral Effect of ID45 and Increases CVB3-Induced Cell Death.** We have shown that activation of Nrf2 is an important step toward cell survival and inhibition of CVB3 replication. Thus, we reasoned that inactivation of Nrf2 signaling would sensitize cells to CVB3-induced cell apoptosis. To verify this speculation, HeLa cells were transfected with Nrf2 siRNAs, treated with ID45, and then infected with CVB3. Western analysis using cell lysates showed that Nrf2 siRNAs suppressed expression of Nrf2 and its target gene NQO1 compared to the controls (Supplementary Figure S7A). This suppression in CVB3-infected cells in turn inhibited VP1 production. This phenomenon is largely due to the host cell death induced by Nrf2 siRNAs, which could not support CVB3 replication. This notion is further supported by the activation of caspase-3, up-regulation of pro-apoptotic transcription factor CHOP (C/EBP homologous protein), decrease of cell viability (Supplementary Figure S7B), and increase of CVB3 particle release from the dead cells (Supplementary Figure S7C). These data confirmed that the antiviral effect of ID45 is achieved through enhancing cell viability, which requires the activation of the Nrf2-NQO1 signal cascade.

**ID45-Induced NQO1 Up-regulation Protects eIF4GI from Cleavage and Degradation.** NQO1 has been reported to play a role in regulating mRNA translation via protection of eIF4GI from degradation by the proteasome during oxidative stress.<sup>33</sup> It is also known that intact eIF4GI is required for cap-dependent translation initiation of cellular mRNAs but not for cap-independent translation initiation of picornaviruses<sup>34</sup> and that CVB3 infection shuts down host protein translation by cleavage of eIF4GI by its protease 2A.<sup>24</sup> To further explore the underlying mechanism by which ID45 inhibits CVB3 replication, the role of ID45-induced NQO1 expression in regulating eIF4GI stability during ER stress was analyzed. After treatment of the cells with ID45 followed by infection with CVB3, cellular proteins were used to detect eIF4GI protein. As shown in Figure 7A, when comparing the CVB3-infected samples, the ID45-treated cells (lanes 7 and 8) produced less cleavage/degradation products (100–150 kDa) than the DMSO-treated cells (lanes 3 and 4) at 6–8 h pi, suggesting that ID45 protects eIF4GI from cleavage by CVB3 protease and degradation by proteasomes. The role of NQO1 in enhancing the stability of eIF4GI during CVB3 infection was further supported by an experiment using

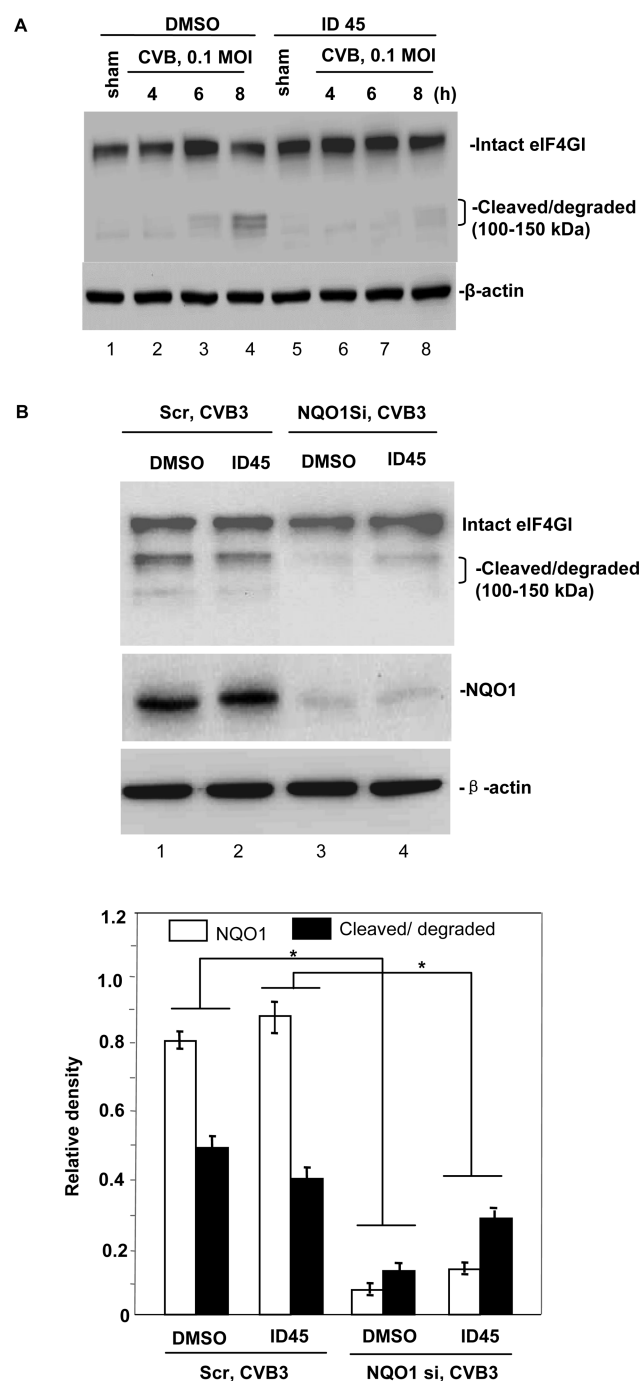


**Figure 7.** ID45-induced NQO1 up-regulation protects eIF4GI from cleavage and degradation. (A) HeLa cells were treated with ID45 and then infected with CVB3 or sham-infected with PBS. Cell lysates collected at indicated time points pi were analyzed for eIF4GI cleavage and degradation by Western blot using 7% SDS-PAGE. The molecular mass markers are indicated.  $\beta$ -Actin was used as a loading control. (B) HeLa cells were transfected with NQO1 siRNA or control siRNA, treated with ID45 or DMSO, and then infected with CVB3. NQO1 expression and eIF4GI cleavage/degradation were detected by Western blot using 10% SDS-PAGE. Levels of NQO1 and cleavage/degradation products were determined by densitometry analysis of data from three independent experiments using the NIH ImageJ program, normalized to  $\beta$ -actin, and presented as mean  $\pm$  SD.  $p < 0.05$  (lower panel).

NQO1 siRNAs. Figure 7B demonstrates that transfection with NQO1 siRNA led to more cleavage and further degradation of the cleaved fragments (i.e., fewer 100–150 kDa fragments) of

eIF4GI than the scrambled siRNA-transfected group. Note that in order to clearly show the cleavage/degradation products, a more concentrated gel (10%) was used in Figure 7B. Our data, to the best of our knowledge, provide the link for the first time between the up-regulation of Nrf2 and anti-CVB3 activity. In general, promotion of host cell survival will create favorable conditions for viral replication. However, in our experimental system, surprisingly Nrf2-mediated cell survival led to strong inhibition of CVB3 replication. In revealing this unique mechanism, our data show that the antiviral effect is attributed to the up-regulation of Nrf2 target gene NQO1 and to the unique structure of CVB3 RNA. It has been reported that NQO1, through the reduction of intracellular quinones, plays a role in the cellular response to oxidative stress.<sup>35</sup> It is also known that NQO1 protein expression protects eIF4GI from degradation by the proteasome. This protection mechanism relies on the interaction of NQO1 and eIF4GI, which blocks the access of proteasome to eIF4GI.<sup>33</sup> eIF4GI is a critical component of the eukaryotic translation initiation complex eIF4F, which serves as a scaffolding protein for the assembly of eIF4F, which is composed of eIF4E (the mRNA cap-binding protein) and eIF4A (an ATPase-dependent RNA helicase). Thus, via its association with the mRNA cap-binding protein eIF4E and with other translation initiation factors (e.g., eIF3) that are bound to the 40S ribosomal subunit, eIF4GI creates a physical link between the cap structure and the ribosome, thus facilitating cap-dependent translation initiation of host cellular mRNAs.<sup>36</sup> eIF4GI also functions in cap-independent (IRES-driven) translation initiation, but this function is carried out by its cleavage forms. Upon infection, eIF4GI is attacked by viral proteases. The resulting eIF4GI cleavage products serve to reprogram the cell's translation machinery, as the N-terminal product inhibits cap-dependent translation of host cell mRNAs by sequestering eIF4E while the C-terminal product stimulates IRES-mediated translation initiation of viral RNAs.<sup>37</sup> CVB3 RNA, like that of other picornaviruses, does not have a cap structure at its 5' end but contains an IRES within the long 5' UTR. Thus CVB3 translation initiation is driven by an IRES mechanism. For this reason, virus RNAs and host mRNAs will compete with each other for translational machineries. However, during treatment with ID45, the up-regulated NQO1 can interact with eIF4GI and protect it from degradation by proteasomes. Interestingly, we found that this interaction protects eIF4GI from cleavage by CVB3 proteases. The stabilized intact eIF4GI then maintains high protein translation rates for host mRNAs and therefore limits cap-independent translation of viral RNAs, which contributes to the antiviral effect of ID45.

In summary, this study has identified a new anti-CVB3 compound, which inhibits CVB3 replication through a previously undocumented novel mechanism (Figure 8). Since the inhibition of CVB3 replication is achieved via suppression of cap-independent translation initiation of viral RNA, ID45 has the potential capability to inhibit other members of picornaviruses as they all utilize the IRES-mediated mechanisms for initiating protein synthesis. In addition, as the induced activation of Nrf2 and up-regulation of its target gene NQO1 are pro-survival markers for the host but not for CVB3, the detection of these markers may serve as a suitable model system for screen of noncytotoxic broad-spectrum antiviral agents for picornaviruses.

## METHODS

**Virus and Cells.** CVB3 (Kandolf strain) was propagated in HeLa cells. The virus stock was isolated from cells by three cycles of freeze–

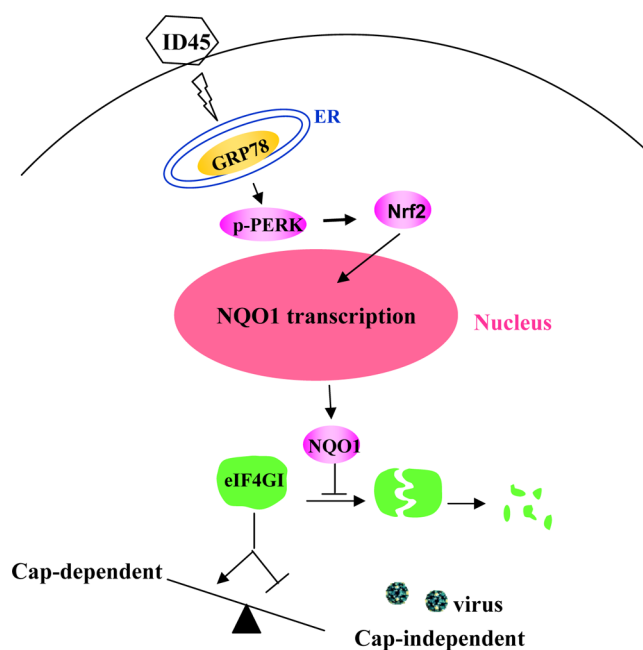


**Figure 8.** Proposed mechanism of ID45 action. Compound ID45 causes GRP78-mediated ER stress response, leading to phosphorylation of PERK, up-regulation and nuclear translocation of transcription factor Nrf2, and subsequent up-regulation of target gene NQO1. The produced NQO1 protein protects eIF4GI from cleavage by viral protease and degradation by proteasomes. The enhanced stability of eIF4GI promotes cap-dependent translation of host mRNAs but suppresses cap-independent translation of coxsackievirus.

thaw followed by centrifugation to remove cell debris and was stored at  $-80^{\circ}\text{C}$ . HeLa cells (ATCC), a cell line that has been well established to study CVB3 pathogenesis, were grown in Dulbecco's modified Eagle's medium (DMEM) supplemented with 100  $\mu\text{g}/\text{mL}$  penicillin-streptomycin, 2 mM glutamine, and 10% Clontech fetal bovine serum (FBS). The HL-1 cell line, a cardiac muscle cell line established from an AT-mouse atrial cardiomyocyte tumor lineage, was a gift from Dr. William C. Claycomb (Louisiana State University Medical Centre, New Orleans, USA).<sup>38</sup> The cells were maintained in Claycomb medium (JRH Biosciences) supplemented with 10% FBS, 100  $\mu\text{g}/\text{mL}$  penicillin-streptomycin, 0.1 mM norepinephrine (Sigma), and 2 mM L-glutamine (Invitrogen).

**Isatin Derivative Synthesis.** The synthesis of the compounds and confirmation of the ID45 structure were conducted by following methods described previously.<sup>39</sup> 5,7-Dibromoindoline-2,3-dione (A, 3.0 g, 9.8 mmol) and anhydrous potassium carbonate (1.25 g, 9 mmol) were added to 40 mL of DMF in a 100 mL flask, and then the mixture was stirred for 1 h at  $65^{\circ}\text{C}$ . Next, *m*-fluorobenzyl chloride (B, 1.72 g, 12 mmol) was added, and the reactant solution was stirred for 4 h at the same temperature. Water (50 mL) was added, and the mixture was filtered and washed with cold water. Red crystals were collected and dried to give 5,7-dibromo-1-(3-fluoro-benzyl)-indole-2,3-dione (C, 3.25 g, yield 80%).  $^1\text{H}$  NMR ( $\text{CDCl}_3$ , 400 MHz):  $\delta$  7.831 (s, 1H, isatin-ArH), 7.739 (s, 1H, isatin-ArH), 7.314 (m, 1H, isatin-ArH and ArH), 7.066–6.932 (m, 3H, isatin-ArH and ArH), 5.400 (s, 2H, Ar- $\text{CH}_2\text{N}$ ).

5,7-Dibromo-1-(3-fluoro-benzyl)-indole-2,3-dione (C, 2.1 g, 5 mmol) was mixed with 2-fluorobenzohydrazide (D, 0.77 g, 5 mmol) and acetic acid (2.5 mL). The mixture was refluxed for 6 h before being cooled to RT. The target compound was filtered, washed with water, and dried to give a crude orange product. Recrystallization from ethanol yielded an orange solid, 2-fluoro-benzoic acid [5,7-dibromo-1-(3-fluoro-benzyl)-2-oxo-1,2-dihydro-indol-3-ylidene]-hydrazide (E, yield 77%, mp 242–244  $^{\circ}\text{C}$ ). The same method was used to prepare all of the other analogues of ID45.

**Western Analysis.** Western blotting was performed by standard protocols as described previously<sup>40</sup> with minor modification. Briefly, the

cells were washed with cold PBS before the addition of the lysis buffer. After incubation for 20 min on ice, the supernatant containing the proteins was collected by centrifugation at  $15,000 \times g$  for 15 min at  $4^\circ\text{C}$ , and the protein concentration was determined by the Bradford assay (Bio-Rad). Equal amounts of protein were separated by 7–10% SDS-polyacrylamide gel electrophoresis (SDS-PAGE) and transferred onto nitrocellulose membranes. The membranes were blocked with PBS containing 0.1% Tween-20 and 5% nonfat dry milk and then probed with one of the following primary antibodies: monoclonal anti-mouse caspas-3, polyclonal anti-mouse histone H1, monoclonal anti-mouse GRP78, polyclonal anti-human Nrf2, polyclonal anti-human Keap1, and monoclonal anti-mouse CHOP from Santa Cruz; polyclonal anti-mouse  $\alpha/\beta$ -tubulin, anti-human p-PERK, anti-human p-eIF2 $\alpha$ , and anti-human total eIF2 $\alpha$  from Cell Signaling; monoclonal anti-mouse NQO1 and polyclonal anti-mouse GCLM from Abcam; monoclonal anti-mouse  $\beta$ -actin from Sigma-Aldrich; or monoclonal anti-mouse VP1 from Leica Microsystems NCL-ENTERO. After washing, each membrane was incubated with a secondary antibody (goat anti-mouse or goat anti-rabbit) conjugated to horseradish peroxidase. Signals were detected by the ECL method according to the manufacturer's instructions (Amersham).

**Virus Plaque Assay.** Virus titers were determined by plaque assay as described previously.<sup>41</sup> Briefly, HeLa cells were seeded onto 6-well plates ( $8 \times 10^5$  cells/well) and incubated at  $37^\circ\text{C}$  for 20 h. When the cell confluence reached approximately 90%, cells were washed with PBS and then overlaid with 500  $\mu\text{L}$  of diluted viral supernatant. The cells were incubated at  $37^\circ\text{C}$  for 60 min, and the supernatant was removed. Finally, cells were overlaid with 2 mL of sterilized soft Bacto-agar-minimal essential medium. The cells were cultured at  $37^\circ\text{C}$  for 72 h, fixed with Carnoy's fixative for 30 min, and stained with 1% crystal violet. The plaques were counted, and the plaque forming unit per milliliter (pfu/mL) was calculated.

**Cell Viability Assay.** Cell viability assays were conducted by using a 3-(4,5-dimethylthiazol-2-yl)-5-(3-carboxymethoxyphenyl)-2-(4-sulfonylphenyl)-2H-tetrazolium salt (MTS) assay kit (Promega) following the manufacturer's instructions. Briefly, cells were incubated with MTS solution for 4 h, and the absorbance was measured at 492 nm using an enzyme-linked immunosorbent assay (ELISA) plate reader (TECAN). The absorbance of nontreated and sham-infected cells was defined as the value of 100% survival (control), and the remaining data were converted to a percentage of the control.

**Nuclear and Cytosolic Protein Extraction.** These proteins were extracted by using a NE-PER nuclear and cytoplasmic extraction kit (Pierce) according to the manufacturer's instructions. Briefly, the cells were treated with ID45 at a dose of  $10 \mu\text{M}$  overnight, washed with cold PBS, and harvested by centrifugation of the collected cell suspensions. The cell pellet was dissolved in Buffer 1 provided in the kit by strong vortex, followed by incubation on ice. After incubation, cells were resuspended in Buffer 2 by vortex and incubating. The cell suspension was centrifuged at  $5,000 \times g$  for 5 min to collect the supernatant containing cytosolic proteins, and the resulting pellet was used for nuclear protein extraction. The pellet was resuspended in buffer NER by vortex. After centrifugation at  $16,000 \times g$  for 10 min, the supernatant was collected for nuclear proteins.

**Immunocytochemistry and Confocal Microscopy.** HeLa cells proliferating on glass coverslips in a 6-well plate at 70% confluence were treated with ID45 at  $10 \mu\text{M}$  for 16 h and then washed with PBS. The cells were stained according to methods described previously.<sup>42</sup> The cells were fixed with 4% paraformaldehyde, permeabilized with 0.1% Triton-X-100 for 10 min, and stained with an anti-Nrf2 primary antibody and then with a goat anti-mouse IgG labeled with green-fluorescent Alexa Fluor 488 dye (Invitrogen). Nuclei were stained with 4',6'-diamidino-2'-phenylindole dihydrochloride (DAPI). Cells were observed under a Leica SP2 AOBs confocal fluorescence microscope.

**siRNAs and Transfection.** All siRNAs (Santa Cruz) used in this study were transfected with oligofectamine using a kit from Invitrogen. Briefly,  $2 \times 10^5$  cells were grown at  $37^\circ\text{C}$  overnight in 6-well plates containing serum-free DMEM. When the cells reached 60–70% confluence, they were washed with  $1 \times$  PBS and overlaid with transfection complexes containing siRNAs and oligofectamine. At 6 h

post transfection the medium was replaced with serum-containing DMEM and the cells were continually cultured for 24 h.

**Statistic Analysis.** Student's *t* test was employed to analyze the data. The results are expressed as means  $\pm$  standard deviations of three independent experiments. A *p* value of less than 0.05 was considered statistically significant.

## ■ ASSOCIATED CONTENT

### Supporting Information

Detailed methods, supplementary figures, and NMR spectra. This material is available free of charge via the Internet at <http://pubs.acs.org>.

## ■ AUTHOR INFORMATION

### Corresponding Authors

\*E-mail: [nkwjg@nankai.edu.cn](mailto:nkwjg@nankai.edu.cn).

\*E-mail: [lzhang03@gmail.com](mailto:lzhang03@gmail.com).

\*E-mail: [decheng.yang@hli.ubc.ca](mailto:decheng.yang@hli.ubc.ca).

### Author Contributions

<sup>¶</sup>These two authors contribute equally to this work.

### Notes

The authors declare no competing financial interest.

## ■ ACKNOWLEDGMENTS

This work was supported by the China-Canada Joint Health Research Initiative grants (30911120483) and in part by China National Funds for Distinguished Young Scientists (31125002), the National Program on Key Basic Research Project (973 program, 2013CB734000), Canada Institute of Health Research (DC0190GP), National Great New Drug Research and Development Project (No. 2011ZX09102-011-11), and Key Natural Science Foundation from Tianjin S&T (No. 12JCZDJC25700). M.G.H. is a recipient of the CIHR-IMPACT and Heart & Stroke Foundation of Canada postdoctoral fellowship. X.Y. is a recipient of the UGF Award of University of British Columbia. We would like to thank G. Fung and D. Kayra for their assistance on confocal microscopy and C. Vavricka for his comments on the manuscript.

## ■ REFERENCES

- (1) Sagar, S., Liu, P. P., and Cooper, L. T., Jr. (2012) Myocarditis. *Lancet* 379, 738–747.
- (2) Aguado, L., Thibaut, H. J., Priego, E. M., Jimeno, M. L., Camarasa, M. J., Neyts, J., and Perez-Perez, M. J. (2010) 9-Arylpurines as a novel class of enterovirus inhibitors. *J. Med. Chem.* 53, 316–324.
- (3) Ji, X. Y., Zhong, Z. J., Xue, S. T., Meng, S., He, W. Y., Gao, R. M., Li, Y. H., and Li, Z. R. (2010) Synthesis and antiviral activities of synthetic glutarimide derivatives. *Chem. Pharm. Bull.* 58, 1436–1441.
- (4) Zhang, L. X., An, R., Wang, J. P., Sun, N., Zhang, S., Hu, J. C., and Kuai, J. (2005) Exploring novel bioactive compounds from marine microbes. *Curr. Opin. Microbiol.* 8, 276–281.
- (5) Zhang, L., Yan, K., Zhang, Y., Huang, R., Bian, J., Zheng, C., Sun, H., Chen, Z., Sun, N., An, R., Min, F., Zhao, W., Zhuo, Y., You, J., Song, Y., Yu, Z., Liu, Z., Yang, K., Gao, H., Dai, H., Zhang, X., Wang, J., Fu, C., Pei, G., Liu, J., Zhang, S., Goodfellow, M., Jiang, Y., Kuai, J., Zhou, G., and Chen, X. (2007) High-throughput synergy screening identifies microbial metabolites as combination agents for the treatment of fungal infections. *Proc. Natl. Acad. Sci. U.S.A.* 104, 4606–4611.
- (6) Wang, Q., Song, F., Xiao, X., Hung, P., Li, L., Monte, A., Abdel-Mageed, W. M., Wang, J., Guo, H., He, W., Xie, F., Dai, H., Liu, M., Chen, C., Xu, H., Liu, M., Piggott, A. M., Liu, X., Capon, R. J., and Zhang, L. (2013) Abyssomicins from a South China Sea deep-sea sediment *Verrucosipora* sp.: Natural thioether Michael addition adducts as potential antitubercular produgs. *Angew. Chem., Int. Ed.*, 1231–1234.

- (7) Klump, W. M., Bergmann, I., Muller, B. C., Ameis, D., and Kandolf, R. (1990) Complete nucleotide sequence of infectious Coxsackievirus B3 cDNA: two initial 5' uridine residues are regained during plus-strand RNA synthesis. *J. Virol.* **64**, 1573–1583.
- (8) Yang, D., Wilson, J. E., Anderson, D. R., Bohunek, L., Cordeiro, C., Kandolf, R., and McManus, B. M. (1997) In vitro mutational and inhibitory analysis of the cis-acting translational elements within the 5' untranslated region of coxsackievirus B3: potential targets for antiviral action of antisense oligomers. *Virology* **228**, 63–73.
- (9) Yang, D., Cheung, P., Sun, Y., Yuan, J., Zhang, H., Carthy, C. M., Anderson, D. R., Bohunek, L., Wilson, J. E., and McManus, B. M. (2003) A shine-dalgarno-like sequence mediates in vitro ribosomal internal entry and subsequent scanning for translation initiation of coxsackievirus B3 RNA. *Virology* **305**, 31–43.
- (10) Kaufman, R. J. (1999) Stress signaling from the lumen of the endoplasmic reticulum: coordination of gene transcriptional and translational controls. *Genes Dev.* **13**, 1211–1233.
- (11) Qian, Z., Xuan, B., Chapa, T. J., Gualberto, N., and Yu, D. (2012) Murine cytomegalovirus targets transcription factor ATF4 to exploit the unfolded protein response. *J. Virol.* **88**, 6712–6723.
- (12) Ambrose, R. L., and Mackenzie, J. M. (2013) ATF6 signaling is required for efficient West Nile virus replication by promoting cell survival and inhibition of innate immune responses. *J. Virol.* **87**, 2206–2214.
- (13) Jezequel, A. M., and Steiner, J. W. (1966) Some ultrastructural and histochemical aspects of Coxsackie virus-cell interactions. *Lab. Invest.* **15**, 1055–1083.
- (14) Li, J., and Lee, A. S. (2006) Stress induction of GRP78/BiP and its role in cancer. *Curr. Mol. Med.* **6**, 45–54.
- (15) Wu, J., Rutkowski, D. T., Dubois, M., Swathirajan, J., Saunders, T., Wang, J., Song, B., Yau, G. D., and Kaufman, R. J. (2007) ATF6 $\alpha$  optimizes long-term endoplasmic reticulum function to protect cells from chronic stress. *Dev. Cell* **13**, 351–364.
- (16) Harding, H. P., Zhang, Y., and Ron, D. (1999) Protein translation and folding are coupled by an endoplasmic-reticulum-resident kinase. *Nature* **397**, 271–274.
- (17) Shi, Y., Vattem, K. M., Sood, R., An, J., Liang, J., Stramm, L., and Wek, R. C. (1998) Identification and characterization of pancreatic eukaryotic initiation factor 2  $\alpha$ -subunit kinase, PEK, involved in translational control. *Mol. Cell Biol.* **18**, 7499–7509.
- (18) Cullinan, S. B., Zhang, D., Hannink, M., Arvisais, E., Kaufman, R. J., and Diehl, J. A. (2003) Nrf2 is a direct PERK substrate and effector of PERK-dependent cell survival. *Mol. Cell Biol.* **23**, 7198–7209.
- (19) Zhang, H. M., Ye, X., Su, Y., Yuan, J., Liu, Z., Stein, D. A., and Yang, D. (2010) Coxsackievirus B3 infection activates the unfolded protein response and induces apoptosis through downregulation of p58IPK and activation of CHOP and SREBP1. *J. Virol.* **84**, 8446–8459.
- (20) Gilturmes, M. S., Hay, M. E., and Fenical, W. (1989) Symbiotic marine-bacteria chemically defend crustacean embryos from a pathogenic fungus. *Science* **246**, 116–118.
- (21) Quenelle, D. C., Keith, K. A., and Kern, E. R. (2006) In vitro and in vivo evaluation of isatin-beta-thiosemicarbazone and marboran against vaccinia and cowpox virus infections. *Antiviral Res.* **71**, 24–30.
- (22) Kang, I. J., Wang, L. W., Hsu, T. A., Yueh, A., Lee, C. C., Lee, Y. C., Lee, C. Y., Chao, Y. S., Shih, S. R., and Chern, J. H. (2011) Isatin-beta-thiosemicarbazones as potent herpes simplex virus inhibitors. *Bioorg. Med. Chem. Lett.* **21**, 1948–1952.
- (23) Medvedev, A., Buneeva, O., and Glover, V. (2007) Biological targets for isatin and its analogues: Implications for therapy. *Biol. Targets Ther.* **1**, 151–162.
- (24) Chau, D. H., Yuan, J., Zhang, H., Cheung, P., Lim, T., Liu, Z., Sall, A., and Yang, D. (2007) Coxsackievirus B3 proteases 2A and 3C induce apoptotic cell death through mitochondrial injury and cleavage of eIF4GI but not DAPS/p97/NAT1. *Apoptosis* **12**, 513–524.
- (25) Harding, H. P., Zhang, Y., Zeng, H., Novoa, I., Lu, P. D., Calfon, M., Sadri, N., Yun, C., Popko, B., Paules, R., Stojdl, D. F., Bell, J. C., Hettmann, T., Leiden, J. M., and Ron, D. (2003) An integrated stress response regulates amino acid metabolism and resistance to oxidative stress. *Mol. Cell* **11**, 619–633.
- (26) Harding, H. P., Novoa, I., Zhang, Y., Zeng, H., Wek, R., Schapira, M., and Ron, D. (2000) Regulated translation initiation controls stress-induced gene expression in mammalian cells. *Mol. Cell* **6**, 1099–1108.
- (27) Cullinan, S. B., and Diehl, J. A. (2004) PERK-dependent activation of Nrf2 contributes to redox homeostasis and cell survival following endoplasmic reticulum stress. *J. Biol. Chem.* **279**, 20108–20117.
- (28) Itoh, K., Wakabayashi, N., Katoh, Y., Ishii, T., Igarashi, K., Engel, J. D., and Yamamoto, M. (1999) Keap1 represses nuclear activation of antioxidant responsive elements by Nrf2 through binding to the amino-terminal Neh2 domain. *Genes Dev.* **13**, 76–86.
- (29) Kwon, J., Han, E., Bui, C. B., Shin, W., Lee, J., Lee, S., Choi, Y. B., Lee, A. H., Lee, K. H., Park, C., Obin, M. S., Park, S. K., Seo, Y. J., Oh, G. T., Lee, H. W., and Shin, J. (2012) Assurance of mitochondrial integrity and mammalian longevity by the p62-Keap1-Nrf2-Nqo1 cascade. *EMBO Rep.* **13**, 150–156.
- (30) Chan, K., and Kan, Y. W. (1999) Nrf2 is essential for protection against acute pulmonary injury in mice. *Proc. Natl. Acad. Sci. U.S.A.* **96**, 12731–12736.
- (31) Lee, J. M., Shih, A. Y., Murphy, T. H., and Johnson, J. A. (2003) NF-E2-related factor-2 mediates neuroprotection against mitochondrial complex I inhibitors and increased concentrations of intracellular calcium in primary cortical neurons. *J. Biol. Chem.* **278**, 37948–37956.
- (32) Schaedler, S., Krause, J., Himmelsbach, K., Carvajal-Yepes, M., Lieder, F., Klingel, K., Nassal, M., Weiss, T. S., Werner, S., and Hildt, E. (2010) Hepatitis B virus induces expression of antioxidant response element-regulated genes by activation of Nrf2. *J. Biol. Chem.* **285**, 41074–41086.
- (33) Alard, A., Fabre, B., Anesia, R., Marboeuf, C., Pierre, P., Susini, C., Bousquet, C., and Pyronnet, S. (2010) NAD(P)H quinone-oxyl-doreductase 1 protects eukaryotic translation initiation factor 4GI from degradation by the proteasome. *Mol. Cell Biol.* **30**, 1097–1105.
- (34) Jackson, R. J., Hellen, C. U., and Pestova, T. V. (2010) The mechanism of eukaryotic translation initiation and principles of its regulation. *Nat. Rev. Mol. Cell Biol.* **11**, 113–127.
- (35) Moscovitz, O., Tsvetkov, P., Hazan, N., Michaelevski, I., Keisar, H., Ben-Nissan, G., Shaul, Y., and Sharon, M. (2012) A mutually inhibitory feedback loop between the 20S proteasome and its regulator, NQO1. *Mol. Cell* **47**, 76–86.
- (36) Prevot, D., Darlix, J. L., and Ohlmann, T. (2003) Conducting the initiation of protein synthesis: the role of eIF4G. *Biol. Cell* **95**, 141–156.
- (37) Ohlmann, T., Rau, M., Pain, V. M., and Morley, S. J. (1996) The C-terminal domain of eukaryotic protein synthesis initiation factor (eIF) 4G is sufficient to support cap-independent translation in the absence of eIF4E. *EMBO J.* **15**, 1371–1382.
- (38) Claycomb, W. C., Lanson, N. A., Jr., Stallworth, B. S., Egeland, D. B., Delcarpio, J. B., Bahinski, A., and Izzo, N. J., Jr. (1998) HL-1 cells: a cardiac muscle cell line that contracts and retains phenotypic characteristics of the adult cardiomyocyte. *Proc. Natl. Acad. Sci. U.S.A.* **95**, 2979–2984.
- (39) Shang, J. L., Guo, H., Li, Z. S., Ren, B., Li, Z. M., Dai, H. Q., Zhang, L. X., and Wang, J. G. (2013) Synthesis and evaluation of novel sulfenamides as novel anti Methicillin-resistant Staphylococcus aureus agents. *Bioorg. Med. Chem. Lett.* **23**, 724–727.
- (40) Liu, Z., Zhang, H. M., Yuan, J., Lim, T., Sall, A., Taylor, G. A., and Yang, D. (2008) Focal adhesion kinase mediates the interferon-gamma-inducible GTPase-induced phosphatidylinositol 3-kinase/Akt survival pathway and further initiates a positive feedback loop of NF-kappaB activation. *Cell Microbiol.* **10**, 1787–1800.
- (41) Yuan, J., Liu, Z., Lim, T., Zhang, H., He, J., Walker, E., Shier, C., Wang, Y., Su, Y., Sall, A., McManus, B., and Yang, D. (2009) CXCL10 inhibits viral replication through recruitment of natural killer cells in coxsackievirus B3-induced myocarditis. *Circ. Res.* **104**, 628–638.
- (42) Sall, A., Zhang, H. M., Qiu, D., Liu, Z., Yuan, J., Lim, T., Ye, X., Marchant, D., McManus, B., and Yang, D. (2010) Pro-apoptotic activity of mBNIP-21 depends on its BNIP-2 and Cdc42GAP homology (BCH) domain and is enhanced by coxsackievirus B3 infection. *Cell Microbiol.* **12**, 599–614.